International Journal of Minerals, Metallurgy and Materials
Volume 24, Number 12, December 2017, Page 1403
DOI: 10.1007/s12613-017-1533-z

Reinforcing effect of graphene on the mechanical properties of Al_2O_3/TiC ceramics

Zuo-li Li, Jun Zhao, Jia-lin Sun, Feng Gong, and Xiu-ying Ni

Key Laboratory of High Efficiency and Clean Mechanical Manufacture of Ministry of Education, School of Mechanical Engineering, Shandong University, Jinan 250061, China

(Received: 10 April 2017; revised: 14 July 2017; accepted: 9 August 2017)

Abstract: Multilayer graphene (MLG)-reinforced Al_2O_3/TiC ceramics were fabricated through hot pressing sintering, and the reinforcing effect of MLG on the microstructure and mechanical properties of the composites was investigated by experiment and simulation. The simulation of dynamic crack initiation and propagation was investigated based on the cohesive zone method. The results show that the composite added with 0.2wt% MLG has excellent flexural strength and high fracture toughness. The major reinforcing mechanisms are the synergistic effect by strong and weak bonding interfaces, MLG pull-out, and grain refinement resulting from the addition of MLG. In addition, the aggravating of crack deflection, branching, blunting, and bridging have indispensable contribution to the improvement of the as-designed materials.

Keywords: mechanical properties; ceramics; graphene; simulation; interface

1. Introduction

Al_2O_3-based ceramic composites have been universally used in high-speed metal cutting owing to their excellent properties, such as favorable chemical stability and high thermal resistance, hardness, and wear resistance [1–3]. The inherent drawbacks, i.e., brittleness, of these composites cannot be ignored. Some methods have been proposed to reinforce Al_2O_3-based ceramics. The phase transformation of ZrO_2 (from t-phase to m-phase at 950°C) was utilized to generate internal stresses, which could prohibit the propagation of cracks in ceramic matrix [4]. Nanoparticles, such as TiC, TiN, or SiC, are used to pin grain boundaries to refine grains and suppress crack propagation [5–6]. Fiber and whisker also work efficiently to improve the mechanical properties of Al_2O_3-based ceramic composites, and carbon nanotubes (CNTs) are one of the commonly used fibers. Bocanegra-Bernal *et al.* [7] reported that the addition of CNTs improved the fracture toughness by 44%. However, CNTs can easily entangle with one another [8], thereby limiting the toughening effect.

Graphene, which is a monolayer of a sp^2-hybridizer carbon atom and possesses a unique two-dimensional structure, has attracted tremendous attention as candidate reinforcing phase of composites. Graphene has larger specific surface area (2620 m^2/g), higher strength (130 GPa), and lower cost [9] than CNTs, although both exhibit excellent mechanical, thermal, and electrical properties [10].

Multilayer graphene (MLG), which comprises a small number (2–10) of well-defined, countable, stacked graphene layers [11], could be used as an ideal reinforcing phase. MLG with high strengthening and toughening effect could be obtained by incorporating it to pure ceramics. Liu [12] discussed the preparation of MLG/Al_2O_3 ceramics and reported 30.75% enhancement in flexural strength and 27.20% improvement in fracture toughness for 0.78vol% MLG/Al_2O_3 ceramics in comparison with monolithic Al_2O_3 ceramics. Kim *et al.* [13] claimed that the grain growth was remarkably inhibited (~50.4%) by graphene, and the fracture toughness was improved (~21.9%) for Al_2O_3–3wt% graphene composites. Fan *et al.* [14] also found that MLG restrained the grain growth of 1.2vol% MLG/Al_2O_3 ceram-

Corresponding author: Jun Zhao E-mail: zhaojun@sdu.edu.cn

ics, and the grain size of the composite was 10 times finer than that of monolithic Al_2O_3 sintered under identical conditions. Porwal *et al.* [15] discovered that the strengthening effect was degenerated with increasing MLG. Similar results were reported in literatures [16–17]. The toughening mechanisms were the synergistic effect of crack deflection, branching, and bridging induced by MLG [18]. The pull-out of MLG was another mechanism [19–20].

The majority of work on MLG reinforcement has been carried out on pure ceramics. However, pure ceramics, such as Al_2O_3 and Si_3N_4, are seldom used as cutting tool materials. Studies on MLG-reinforced multiphase ceramics are also inadequate. The microstructures of multiphase ceramics are different from those of pure ceramics, so the corresponding reinforcing mechanisms may be different and need to be studied thoroughly. Given the complexity of microstructures, numerical simulation would be an effective method to assist the determination of the effect of the reinforcing mechanisms of MLG on mechanical properties.

In this work, the effects of MLG on the mechanical properties and microstructures of MLG-reinforced Al_2O_3/TiC ceramics were investigated both numerically and experimentally. A finite element method (FEM) model of ceramic composite was developed based on the cohesive element method (CZM) to examine the effect of MLG on crack evolution. MLG-reinforced Al_2O_3/TiC ceramics with different MLG contents were prepared by hot pressing (HP). The mechanical properties (flexural strength and fracture toughness) of these composites were tested, and the reinforcing mechanisms were discussed.

2. Experimental

2.1. Material preparation

The starting powders used included α-Al_2O_3 (500 nm in diameter, purity 99%, Shanghai ST-Nano Science & Technology Co. Ltd., China), TiC (500 nm in diameter, purity 99%, Shanghai ST-Nano Science & Technology Co. Ltd., China), MLG (<10 nm thick and 20 μm in diameter, Jinan Moxi New Material Technology Co. Ltd., China), and MgO as sintering aid. The volume ratio of Al_2O_3, TiC, and MgO was 7:2.9:0.1. Polyvinylpyrrolidone (PVP, Gobekie New Materials Science Technology Co. Ltd., China) was used as the dispersant of MLG. The MLG and PVP contents in the Al_2O_3/TiC ceramics are listed in Table 1. A schematic diagram of the fabrication process is shown in Fig. 1. MLG was dispersed in PVP solution by ultrasonic vibration for 2 h. Al_2O_3, TiC, and MgO were individually dispersed in ethanol. Then all solutions were mixed and dispersed for additional 2 h. The slurry was milled by Al_2O_3 balls (10 mm in diameter) with a speed of 500 r/min and a ball to powder mass ratio of 5:1 for 48 h and dried in a vacuum drying chamber. Finally, the dried composite powder was put into graphite dies of 42 mm in diameter and sintered at 1650°C and 30 MPa.

Table 1. Contents of MLG and PVP in Al_2O_3/TiC ceramics

wt%

Sample	ATS0	ATS1	ATS2	ATS3	ATS4	ATS5
MLG	0	0.1	0.2	0.3	0.4	0.5
PVP	0	0.075	0.150	0.225	0.300	0.375

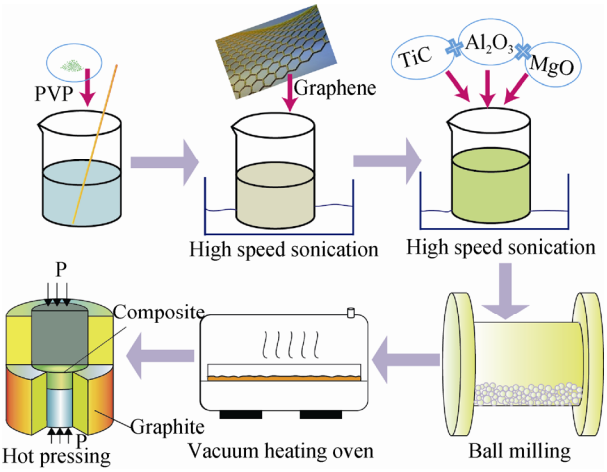

Fig. 1. Schematic diagram of the material fabrication process.

2.2. Specimen processing

The sintered compact was cut into bars with a dimension of 3.25 mm × 4.25 mm × 30 mm by a wire cutting machine. The bars were chamfered with a dimension of about 0.1 mm × 0.1 mm to avoid machining flaws. The bar surfaces were ground with an MQ6025A-type universal tool grinder. The final bars had a dimension of 3 mm × 4 mm × 30 mm. Flexural strength was measured by the three-point bending method in a WDW-50E tester (China). A Vickers hardness tester (Model MHVD-30AP, China) was used to measure Vickers hardness with a critical load of 196 N and a lasting time of 15 s. The fracture toughness of the composites was obtained by the indentation method [21], and the densities were measured with an analytical balance (Model AuY120, Japan). A scanning electron microscope (SEM, QUANTA FEG-250, FEI Inc., USA) was employed to analyze the fractured surfaces and indentation cracks.

3. Numerical simulation procedure

A two-dimensional microstructure model consisting of

1000 grains was constructed by Voronoi tessellations, and the material properties of Al_2O_3 and TiC were proportionately assigned to these tessellations, as shown in Fig. 2(a). The yellowish-brown portions represented Al_2O_3, and the blue part was TiC. Zero-thickness cohesive elements were embedded along the grain boundary and inside the grain interior by a code written with C language. The cohesive elements representing MLG are labeled by red lines, and other elements along the phase interfaces are labeled by dark blue lines, as shown in Fig. 2(b). The distribution of MLG was random, and its quantity was controllable. Vertical dynamic tension force was applied to the upper boundary of the model, and the lower boundary was constrained. The material parameters are given in Table 2. The interfacial strength parameters were $T_{TiC/TiC}$ = 200 MPa, $T_{Al2O3/Al2O3}$ =240 MPa, and $T_{Al2O3/TiC}$ =220 MPa, and the fracture energy was computed by the following equation [22]:

$$G = \left[\left(1-\nu^2\right)/E\right]K_{IC}^2 \quad (1)$$

where G is the fracture energy, J/mm^2; K_{IC} is the fracture toughness, MPa·m$^{1/2}$; E is the Young's modulus, GPa; and v is the Poisson's ratio. Plane strain conditions and maximum principal stress criterion were considered. Within the framework of the cohesive elements, the dynamic crack initiation and propagation processes under external force loading were simulated. The strain energy and the dissipation energy during the fracture process were set as the output data for the simulation.

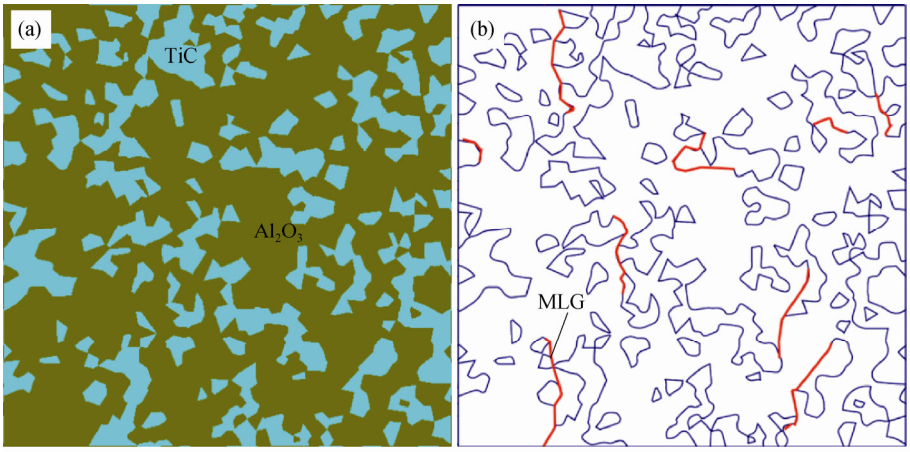

Fig. 2. Numerical microstructure after assigning material properties (a) and cohesive elements along the interfaces (b) (The red lines represent MLG).

Table 2. Material parameters of the simulation model

Material	Density, ρ / (g·cm^{-3})	Young's modulus, E / GPa	Poisson's ratio, v	Fracture toughness, K_{IC} / (MPa·m$^{1/2}$)	Tensile strength / MPa
Al_2O_3 [23]	3.97	394	0.27	4.5	300
TiC [24]	4.94	450	0.18	5.36	258
MLG [25–26]	0.25	1000	0.186	4.0	130000

4. Results and discussion

4.1. Mechanical properties

Fig. 3 illustrates the mechanical properties of the Al_2O_3/TiC ceramics added with different MLG contents. The flexural strength and fracture toughness both initially increased and decreased with increasing MLG content. The results indicated that the addition of an appropriate amount of MLG (0.1wt%–0.3wt%) could enhance the flexural strength and fracture toughness of the composites. The ATS2 sample with 0.2wt% MLG exhibited the highest flexural strength (981.5 MPa) and fracture toughness (6.14 MPa·m$^{1/2}$), which were 31% and 23% higher than those of ATS0, respectively. These properties were also higher than those in CNTs-reinforced Al_2O_3/TiC ceramics (556.19 MPa and 5.0 MPa·m$^{1/2}$, respectively) reported in Refs. [27–28]. Further addition of MLG deteriorated the mechanical properties because of MLG agglomeration according to Kostecki [29]. Moreover, the Vickers hardness of the Al_2O_3/TiC ceramics was slightly improved, and the relative density of all samples was above 98%. The relationship between the mechanical properties and the microstructure was discussed in the following section.

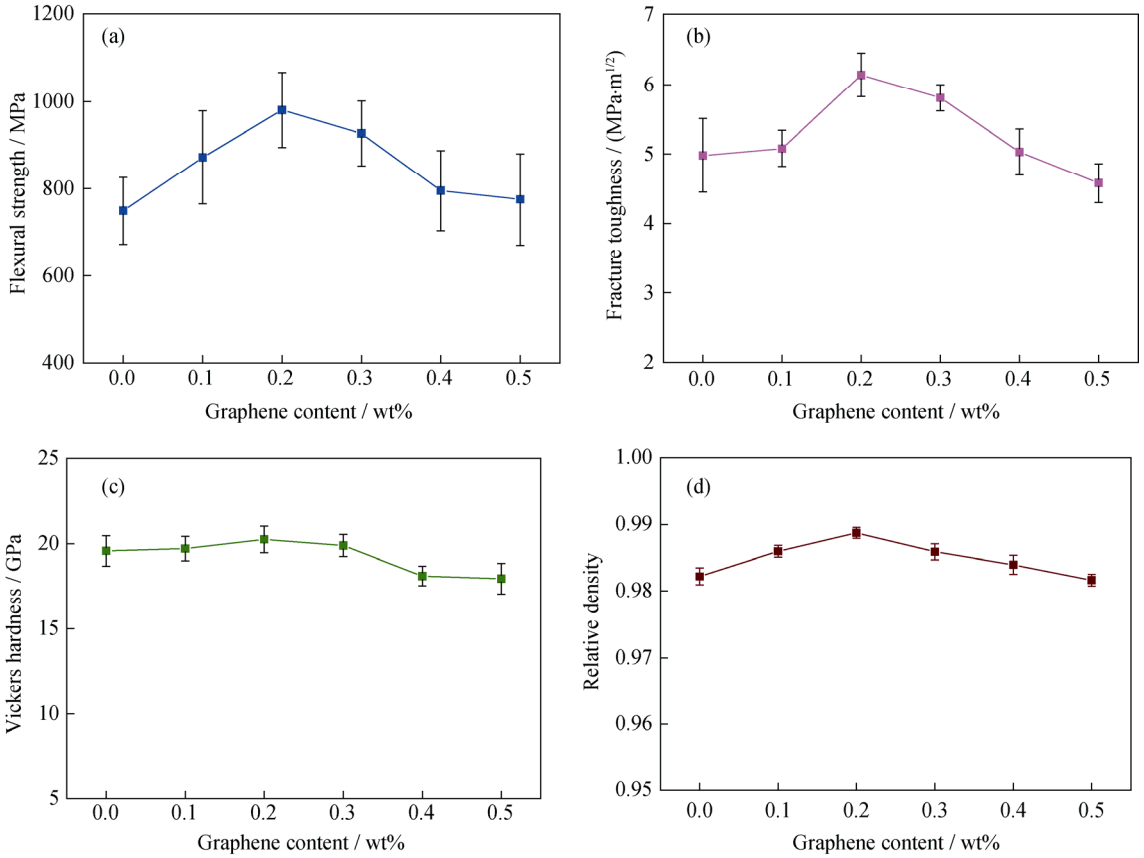

Fig. 3. Effect of MLG content on the mechanical properties of Al_2O_3/TiC ceramics: (a) flexural strength; (b) fracture toughness; (c) Vickers hardness; (d) relative density.

4.2. Microstructure analysis

The mechanical properties of composites depend on their microstructures. The effect of MLG on microstructures is discussed on the basis of flexural fractured surfaces and indentation cracks.

4.2.1. Analysis of the flexural fractured surface

Fig. 4 shows the morphology of the flexural fractured surfaces of the Al_2O_3/TiC ceramics. The composite without MLG exhibited relatively rough surface due to grain pull-out, indicating that the major fracture mode was intergranular. The composites added with MLG showed fairly flush fractured surfaces, and the characteristic river pattern was clearly observed in single particles, indicating that transgranular fracture was the major fracture mode.

The MLG phase was labeled by yellow arrows, as shown in Figs. 4(b)–4(d). The MLG distribution in ATS2 was the most homogeneous among all the samples. As the mass fraction of MLG increased, it agglomerated and formed large clusters, which are marked by yellow boxes in Figs. 4(c) and 4(d). Raman spectrum was used to ascertain the aggregation of MLG in the matrix, and the curves are shown in Fig. 5. The D and G bands of graphene were observed in the two composites, and the intensity ratio of D- Raman peak and G- Raman peak (I_D/I_G ratio) in ATS2 was higher than that in ATS5. Hence, MLG in ATS5 had more layers than that in ATS2 because the ratio decreased as the number of layers increased [30], and the self-assembly of MLG occurred in ATS5. According to the results of the mechanical test, the aggregation of MLG had negative effect on performance improvements of the composites. Consistent with these findings, Ramirez and Osendi [20] discussed that the strengthening effect would decrease once the content of MLG reaches beyond the limit because of its aggregation.

As the MLG content increased, the size of Al_2O_3 increased sharply along the direction parallel to MLG, but the growth in the other direction was obstructed by MLG, as marked by red arrows in Figs. 4(c) and 4(d). This finding was related to the preferred orientation of MLG [31], while MLG was proven to have great ability to restrain particle growth. Hence, improving the uniform distribution of MLG in MLG-reinforced Al_2O_3/TiC multiphase ceramics would be an effective way to refine grain size.

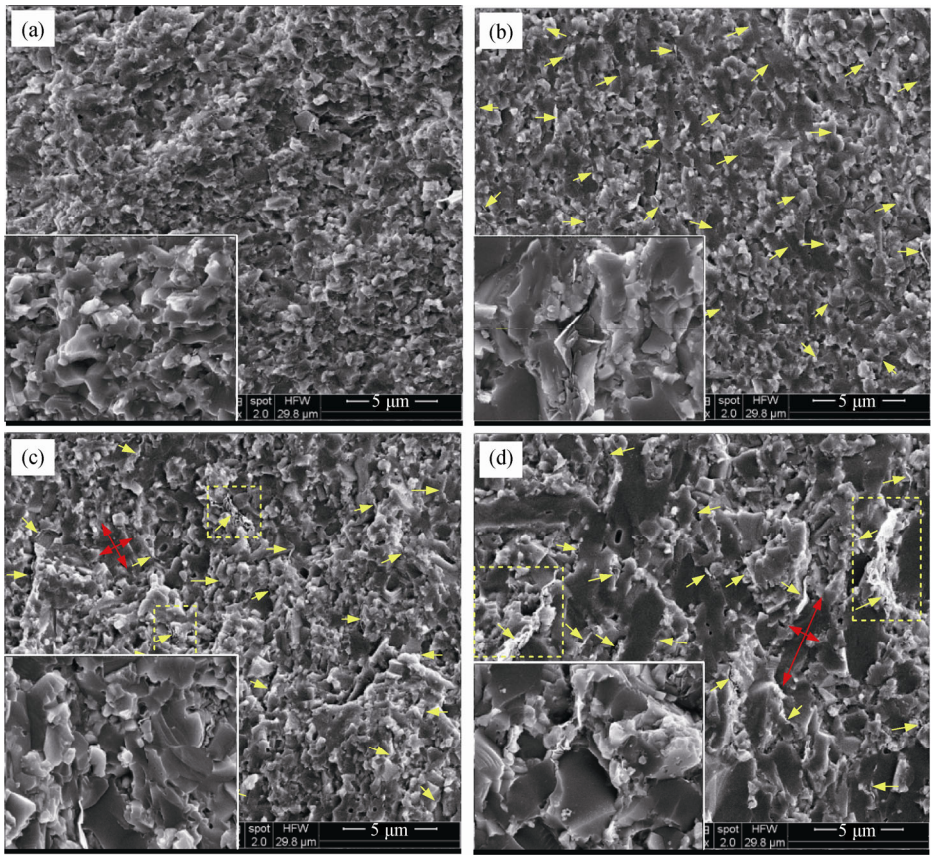

Fig. 4. SEM micrographs of the fractured surfaces of ATS0 (a), ATS2 (b), ATS4 (c), and ATS5 (d). The insets show the high-magnification images of fracture morphology, the yellow arrows label the locations of MLG, the yellow boxes indicate the serious aggregation of MLG, and the red arrows characterize the grain size.

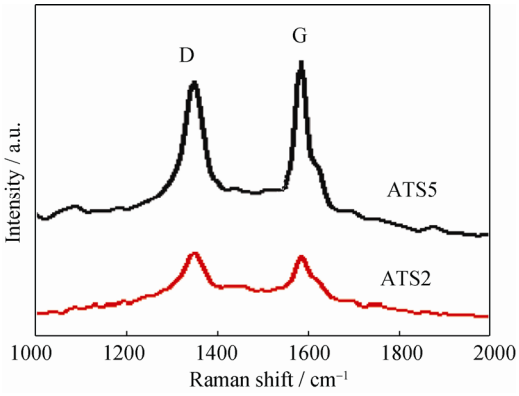

Fig. 5. Raman spectrum of the MLG-reinforced Al_2O_3/TiC ceramics.

4.2.2. Numerical and experimental analyses of crack paths

The dynamic influence of MLG on crack path is difficult to determine by experiments. Numerical simulation is a convenient method used to observe microstructure variations during the fracture processes and investigate the effect of MLG. Numerical results showed that under the ongoing external loading, initial damage appeared at a weak point. Subsequently, micro-cracks initiated and propagated along the direction with minimum gradient of stress field. The external work was transformed to elastic strain energy for microstructure deformation and damage dissipation energy for fracturing. The variations in strain energy and dissipation energy during the fracture processes are shown in Fig. 6. Cracks initiated as the strain energy reached the peak value; thereafter, the dissipation energy increased rapidly and

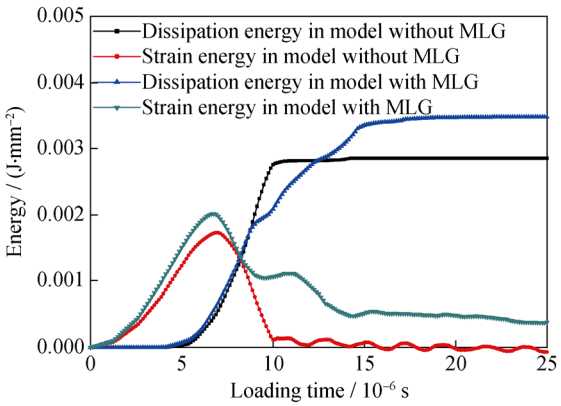

Fig. 6. Energy variation curves during fracture initiation and propagation in Al_2O_3/TiC ceramics.

started to level off as the fracture process was at a stable state. The peak value of strain energy and the maximum dissipation energy in the model with MLG were all higher than those without MLG, indicating that MLG could enhance the resistance of the composites to deformation and destruction. The simulated crack paths are shown in Fig. 7. Despite that multiple cracks initiated and propagated in each model, severe crack deflection appeared in the model with MLG, and crack growth was stopped by MLG.

Fig. 8 shows the indentation crack paths on the polished surfaces. The dark gray phase is Al_2O_3, and the light gray phase is TiC. The influence of MLG on crack morphology was consistent with that observed in the simulation. Unlike the relatively straight path in Fig. 8(a), the crack paths in Figs. 8(b), 8(c), and 8(d) were characterized by crack deflection and branching. The crack usually deviated from its original direction as it encountered MLG and then propagated along MLG. In addition, MLG pull-out and bridging were clearly observed. The included angle between crack and MLG decided the severity of crack deflection. An included angle close to 90° is shown in Fig. 8(c). The original direction of the major crack was nearly perpendicular to

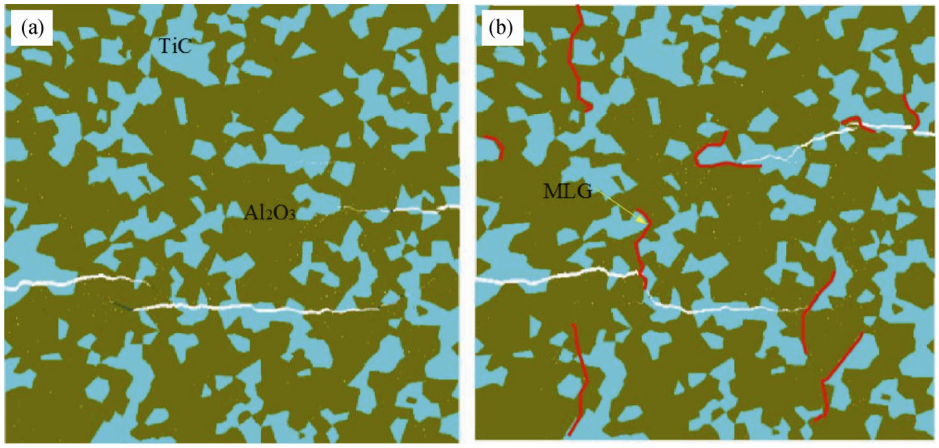

Fig. 7. Simulated crack paths in the Al_2O_3/TiC ceramics without (a) and with (b) MLG.

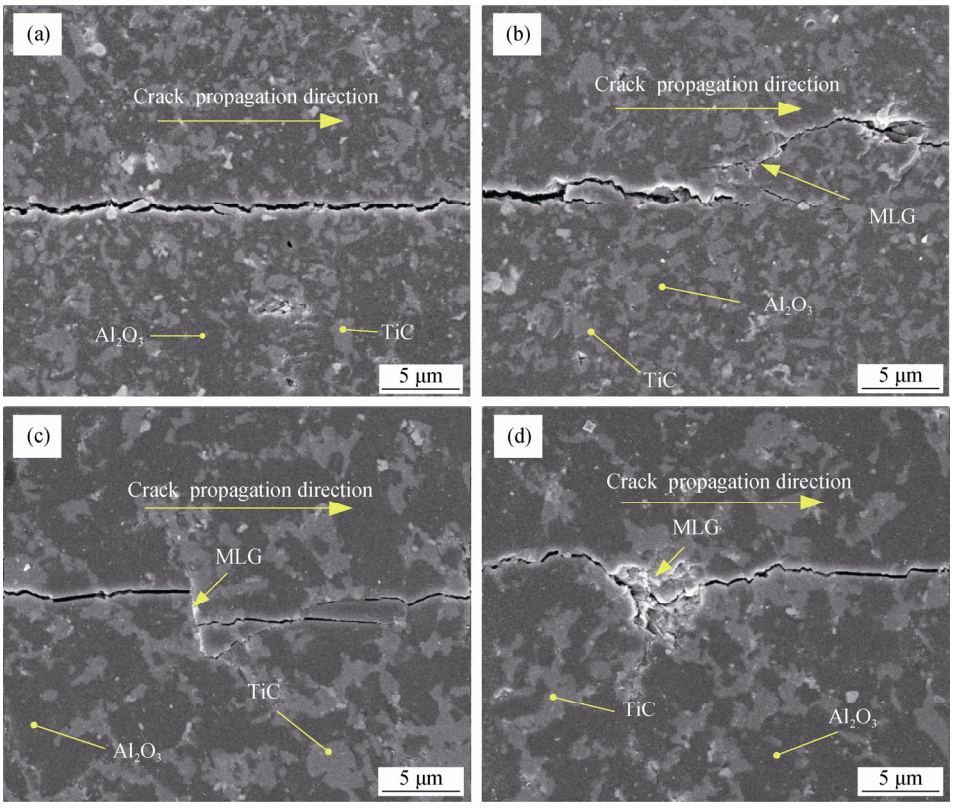

Fig. 8. Indentation crack path in samples ATS0 (a), ATS2 (b), ATS4 (c), and ATS5 (d).

MLG, so it was significantly deflected. In Figs. 8(b) and 8(d), the cracks showed slight deflection for small included angles. These phenomena reasonably explained the enhancement of fracture toughness of the composites. The surface peeling behavior was observed in the composites with MLG addition and became severe as the content of MLG increased (Fig. 9). This finding indicated the increase in the number of weak bonding interfaces between MLG and ceramic phases. The weak bonding interface easily induced microcracks, resulting in microcrack toughening and improved fracture toughness of the composites [32].

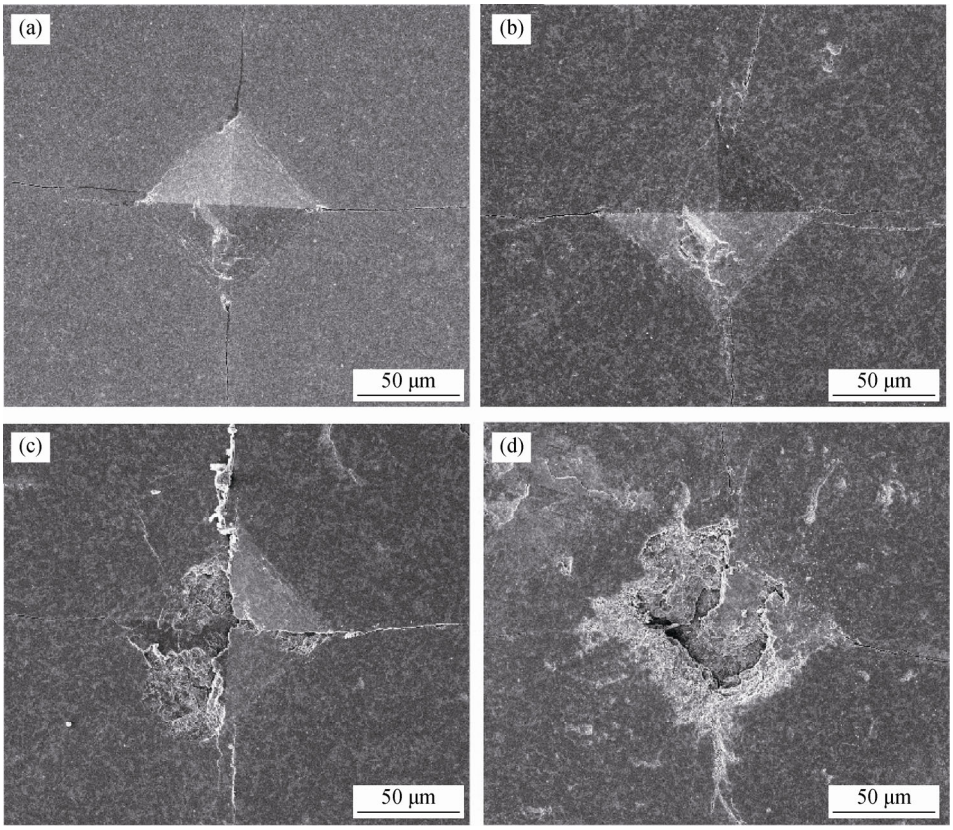

Fig. 9. Indentation micrographs of ceramic samples ATS0 (a), ATS2 (b), ATS4 (c), and ATS5 (d).

4.3. Toughening and strengthening mechanisms

The test results showed that MLG addition contributed to the improvement of the mechanical properties of Al_2O_3/TiC ceramics. The reinforcing mechanisms of MLG can be explained from two aspects: one is the microstructure changes caused by MLG, such as co-existence of strong and weak bonding interfaces and refinement of Al_2O_3 grains; and the other one is the hindering effect of MLG on crack propagation.

Fig. 10(a) shows the strong and weak bonding interfaces observed from the fractured surface of ATS2. Weak bonding interfaces coexisted with strong bonding interfaces, and some local microcracks were found around the weak bonding interfaces. Fig. 10(b) illustrates the corresponding reinforcing mechanisms. MLG became in contact with multiple particles because of its high specific surface area, and resulting in the co-existence of strong and weak bonding interfaces between MLG and ceramic phases. MLG became a link between the strong and weak bonding interfaces, as shown in Fig. 10(b). Under external loading, microcracks easily initiated around the weak bonding interfaces and thus induced microcrack toughening [33]; the strong bonding interfaces maintained sufficient fracture resistance. The toughness of MLG-reinforced Al_2O_3/TiC ceramics improved without decreasing the strength because of the synergistic effect of strong and weak bonding interfaces.

A schematic diagram of MLG affecting the crack propagation path is shown in Fig. 11. MLG has unique mechanical properties (high strength, toughness, and Young's modulus) and, similar to a barrier, hinders the propagation of crack path, leading to enhanced crack deflection, branching, and blunting, which increased the fracture energy of the composites. In addition, the MLG pull-out and bridging increased the fracture resistance and improved the toughness of the composites.

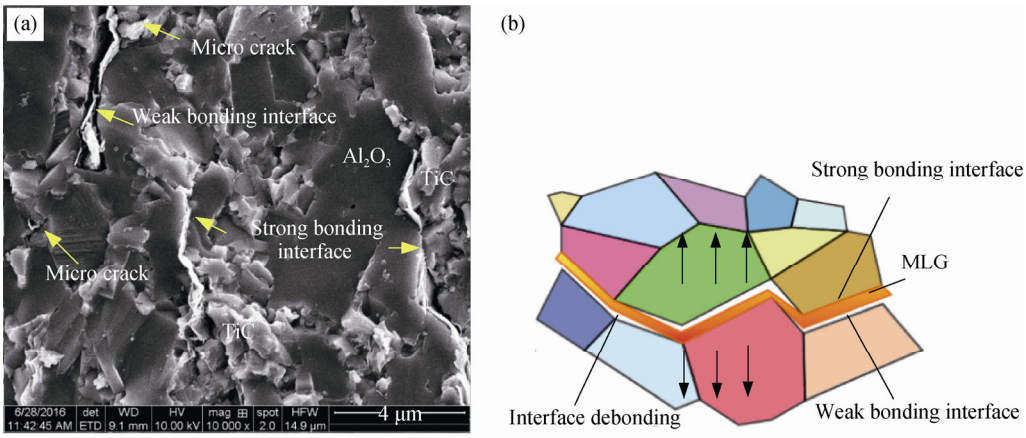

Fig. 10. Strong and weak bonding interfaces: (a) fractured surface; (b) reinforcing mechanism.

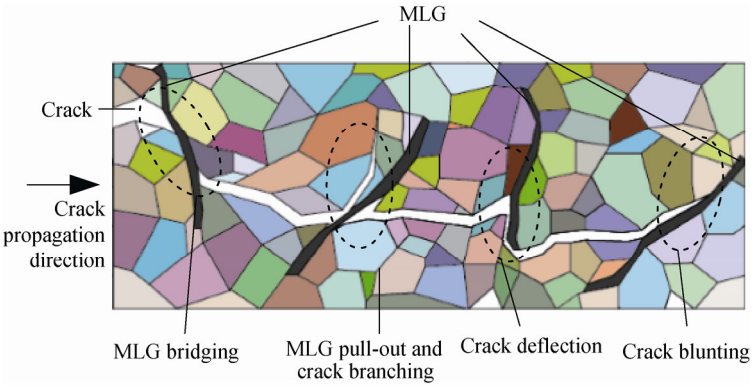

Fig. 11. Schematic graphics of MLG effects on crack propagation in Al_2O_3/TiC ceramics.

MLG is beneficial for reinforcing Al_2O_3/TiC ceramics, but its aggregation produces a barrier effect and causes the accumulation of in-phase particles, leading to the abnormal grain growth in ATS4 and ATS5. Moreover, the grain boundary stress increased, resulting in a decrease in the mechanical properties of the composites.

5. Conclusions

This work fabricated the MLG-reinforced Al_2O_3/TiC ceramics by HP and investigated the reinforcing effect of MLG on the mechanical properties of Al_2O_3/TiC ceramics through numerical simulation and experiment. The following conclusions can be made.

(1) The addition of an appropriate amount of MLG (0.1wt%–0.3wt%) could enhance the flexural strength and fracture toughness of the composites. The Al_2O_3/TiC ceramic added with only 0.2wt% MLG shows the highest flexural strength (981.5 MPa) and fracture toughness (6.14 MPa·$m^{1/2}$).

(2) MLG is an ideal reinforcing phase for Al_2O_3/TiC ceramics to improve their flexural strength and fracture toughness. The reinforcing mechanisms include the synergistic effect induced by strong and weak bonding interfaces, MLG pull-out and bridging, the combination of crack deflection, branching and blunting, and grain refinement.

(3) According to the Raman spectrum analyses and the test results, the self-assembly behavior of MLG deteriorates the dispersion performance of the ceramic matrix and has a negative effect on the mechanical properties. Thus, the content of MLG should be controlled within an appropriate range.

Acknowledgement

This work was financially supported by the National Natural Science Foundation of China (No. 51475273).

References

[1] K. Zimmermann, G.A. Schneider, A.K. Bhattacharya, and W. Hintze, Surface modification of Al_2O_3/TiC cutting ceramics, *J. Am. Ceram. Soc.*, 90(2007), No. 12, p. 3773.

[2] Y.H. Fei, C.Z. Huang, H.L. Liu, and B. Zhou, Mechanical properties of Al_2O_3–TiC–TiN ceramic tool materials, *Ceram. Int.*, 40(2014), No. 7, p. 10205.

[3] K.F. Cai, D.S. Mclachlan, N. Axen, and R. Manyatsa, Preparation, microstructures and properties of Al_2O_3–TiC composites, *Ceram. Int.*, 28(2002), No. 2, p. 217.

[4] W.H. Tuan, R.Z. Chen, T.C. Wang, C.H. Cheng, and P.S. Kuo, Mechanical properties of Al_2O_3/ZrO_2 composites, *J. Eur. Ceram. Soc.*, 22(2002), No. 16, p. 2827.

[5] S.X. Song, X. Ai, J. Zhao, and Q. Wu, Mechanical properties toughening and strengthening mechanisms of Al_2O_3/TiC nanocomposite, *Mater. Mech. Eng.*, 27(2003), No. 12, p. 35.

[6] Z.B. Yin, C.Z. Huang, B. Zou, H.L. Liu, H.T. Zhu, and J. Wang, Preparation and characterization of Al_2O_3/TiC micro–nano-composite ceramic tool materials, *Ceram. Int*., 39(2013), No. 4, p. 4253.

[7] M.H. Bocanegra-Bernal, J. Echeberria, J. Ollo, A. Garcia-Reyes, C. Domínguez-Rios, A. Reyes-Rojas, and A. Aguilar-Elguezabal, A comparison of the effects of multi-wall and single-wall carbon nanotube additions on the properties of zirconia toughened alumina composites, *Carbon*, 49(2011), No. 5, p. 1599.

[8] P. Michelis and J. Vlachopoulos, Complete CNT disentanglement–dispersion–functionalisation in a pulsating micro-structured reactor, *Chem. Eng. Sci.*, 90(2013), No. 10, p. 10.

[9] H. Porwal, S. Grasso, and M.J. Reece, Review of graphene–ceramic matrix composites, *Adv. Appl. Ceram.*, 112(2013), No. 8, p. 443.

[10] X. Jiang and L.T. Drzal, Multifunctional high density polyethylene nanocomposites produced by incorporation of exfoliated graphite nanoplatelets 1: Morphology and mechanical properties, *Polym. Compos.*, 31(2009), No. 6, p. 1091.

[11] A. Bianco, H.M. Cheng, T. Enoki, Y. Gogotsi, R.H. Hurt, N. Koratkar, T. Kyotani, M. Monthioux, C.R. Park, J.M.D. Tascon, and J. Zhang, All in the graphene family – A recommended nomenclature for two-dimensional carbon materials, *Carbon*, 65(2013), No. 6, p. 1.

[12] J. Liu, H.X. Yan, and K. Jiang, Mechanical properties of graphene platelet-reinforced alumina ceramic composites, *Ceram. Int.*, 39(2013), No. 6, p. 6215.

[13] W. Kim, H.S. Oh, and I.J. Shon, The effect of graphene reinforcement on the mechanical properties of Al_2O_3 ceramics rapidly sintered by high-frequency induction heating, *Int. J. Refract. Met. Hard Mater.*, 48(2015), p. 376.

[14] Y. Fan, M. Estili, G. Igarashi, W. Jiang, and A. Kawasaki, The effect of homogeneously dispersed few-layer graphene on microstructure and mechanical properties of Al_2O_3 nanocomposites, *J. Eur. Ceram. Soc.*, 34(2014), No. 2, p. 443.

[15] H. Porwal, P. Tatarko, S. Grasso, J. Khaliq, I. Dlouhý, and M.J. Reece, Graphene reinforced alumina nano-composites, *Carbon*, 64(2013), No. 11, p. 359.

[16] P. Kun, O. Tapasztó, F. Wéber, and C. Balázsi, Determination of structural and mechanical properties of multilayer graphene added silicon nitride-based composites, *Ceram. Int.*, 38(2012), No. 1, p. 211.

[17] K. Jiang, J. Li, and J. Liu, Spark plasma sintering and characterization of graphene platelet/ceramic composites, *Adv. Eng. Mater.*, 17(2015), No. 5, p. 716.

[18] Y. Cheng, Y. Zhang, T.Y. Wan, Z.B. Yin, and J.A. Wang, Mechanical properties and toughening mechanisms of graphene platelets reinforced Al_2O_3/TiC composite ceramic tool materials by microwave sintering, *Mater. Sci. Eng. A*, 680(2017), p. 190.

[19] J. Liu, H.X. Yan, M.J. Reece, and K. Jiang, Toughening of zirconia/alumina composites by the addition of graphene platelets, *J. Eur. Ceram. Soc.*, 32(2012), No. 16, p. 4185.

[20] C. Ramirez and M.I. Osendi, Toughening in ceramics containing graphene fillers, *Ceram. Int.*, 40(2014), No. 7, p. 11187.

[21] M. Sebastiani, K.E. Johanns, E.G. Herbert, and G.M. Pharr, Measurement of fracture toughness by nanoindentation methods: recent advances and future challenges, *Curr. Opin. Solid State Mater. Sci.*, 19(2015), No. 6, p. 324.

[22] I. Benedetti and M.H. Aliabadi, A three-dimensional cohesive-frictional grain-boundary micromechanical model for intergranular degradation and failure in polycrystalline materials, *Comput. Methods Appl. Mech. Eng.*, 265(2013), No. 9, p. 36.

[23] Ferro-Ceramic Grinding Inc., *Ceramic Properties Tables*. http://www.ferroceramic.com/alumina_99_table.htm.

[24] M.L. Bauccio, *ASM Engineered Materials Reference Book,* 2nd Ed, Ohio: ASM international, 1994.

[25] C.G. Lee, X.D. Wei, J.W. Kysar, and J. Hone, Measurement of the elastic properties and intrinsic strength of monolayer graphene, *Science*, 321(2008), No. 5887, p. 385.

[26] P. Zhang, L.L. Ma, F.F. Fan, Z. Zeng, C. Peng, P.E. Loya, Z. Liu, Y.J. Gong, J.N. Zhang, X.X. Zhang, P.M. Ajayan, T. Zhu, and J. Lou, Fracture toughness of graphene, *Nat. Commun.*, 5(2014), No. 4, p. 3782.

[27] J.S. Zhao, *Preparation and Properties of $A1_2O_3$/TiC/CNTs Composites* [Dissertation], Shandong Jianzhu University, Jinan, 2012, p. 21.

[28] S.G. Nyembe, *Improvement of Alumina Mechanical and Electrical Properties using Multi-Walled Carbon Nanotubes and Titanium Carbide as a Secondary Phase* [Dissertation], University of Witwatersrand, Johannesburg, 2013, p. 80.

[29] M. Kostecki, M. Grybczuk, P. Klimczyk, T. Cygan, J. Woźniak, T. Wejrzanowski, L. Jaworska, J. Morgiel, and A. Olszyna, Structural and mechanical aspects of multilayer graphene addition in alumina matrix composites–validation of computer simulation model, *J. Eur. Ceram. Soc.*, 36(2016), No.16, p. 4171.

[30] R. Rao, R. Podila, R. Tsuchikawa, J. Katochet, D. Tishler, A.M. Rao, and M. Ishigami, Effects of layer stacking on the combination Raman modes in graphene, *ACS Nano*, 5(2011), No. 3, p. 1594.

[31] X.L. Meng, C.H. Xu, G.C. Xiao, M.D. Yi, and Y.B. Zhang, Microstructure and anisotropy of mechanical properties of graphene nanoplate toughened Al_2O_3-based ceramic composite, *Ceram. Int.*, 42(2016), No. 14, p. 16090.

[32] Y. Ji and J.A. Yeomans, Processing and mechanical properties of Al_2O_3–5vol% Cr nanocomposites, *J. Eur. Ceram. Soc.*, 22(2002), No. 12, p. 1927.

[33] N. Claussen and J. Steeb, Toughening of ceramic composites by oriented nucleation of microcracks, *J. Am. Ceram. Soc.,* 59(1976), No. 9-10, p. 457.